

Elastic Properties of Hybrid Graphene/Boron Nitride Monolayer

Qing Peng, Amir R. Zamiri and Suvranu De

Department of Mechanical, Aerospace and Nuclear Engineering,

Rensselaer Polytechnic Institute, Troy, NY 12180, U.S.A.

Abstract

Recently hybridized monolayers consisting of hexagonal boron nitride (*h*-BN) phases inside graphene layer have been synthesized and shown to be an effective way of opening band gap in graphene monolayers [1]. In this letter, we report an *ab initio* density functional theory (DFT)-based study of *h*-BN domain size effect on the elastic properties of graphene/boron nitride hybrid monolayers (*h*-BNC). We found both inplane stiffness and longitudinal sound velocity of *h*-BNC linearly decrease with *h*-BN concentration.

Substituting C with B and N atoms in graphene has been shown to be a promising way to improve semiconducting properties of graphene up to some point [2–4]. Hexagonal boron nitride (*h*-BN) and graphene have similar 2D lattice structures but with very different physical properties. Interesting nanostructures can be made by mixing these two structures[5–8].

Recently, a promising method has been reported in which atomistic monolayers have been generated consisting of *h*-BN phases in graphene (*h*-BNC) using a thermal catalytic chemical vapor deposition method [1]. These hybrid monolayers have been shown to have isotropic physical properties which can be tailored by controlling the kinetic factors affecting the *h*-BN domain size within graphene layer. This is different from B-doped or N-doped graphene, where the integrity of the *h*-BN structure is missing.

The electronic band structures of *h*-BNC heterostructures were studied in our previous work [9]. Whileas, the mechanical properties of these heterogenous nanosheet are still unknown. In this letter we modeled the *h*-BN domain size effect as *h*-BN concentration effect and examined the elastic properties of *h*-BNC monolayers as a function of *h*-BN concentration using *ab initio* density functional theory.

The main character of *h*-BN domain in *h*-BNC hybrid structures is the integrity of hexagonal structure of *h*-BN and graphene. Therefore, we modeled the *h*-BN domain in *h*-BNC by maintaining the hexagonal structure of *h*-BN locally (B_3N_3 as a “molecule”) within the system. The *h*-BN domain size effect then can be represented by the *h*-BN concentration in the model. We examined the variation of elastic properties of *h*-BNC monolayers as function of *h*-BN concentration. Five *h*-BNC configurations, in order of *h*-BN concentration, 0%, 25%, 50%, 75% and 100% have been studied, where 0% and 100% corresponding to pure graphene and *h*-BN, respectively. The three other concentrations were selected based on their simplicity and representativeness. The atomic structures of these five configurations (Fig. 1) were determined by the *ab initio* density functional theory.

DFT calculations were carried out with the Vienna Ab-initio Simulation Package (VASP) [10–13] which is based on the Kohn-Sham Density Functional Theory (KS-DFT) [14, 15] with the generalized gradient approximations as parameterized by Perdew, Burke and Ernzerhof (PBE) for exchange-correlation functions [16]. The electrons explicitly included in the calculations are the ($2s^22p^2$) electrons of carbon, the ($2s^22p^1$) electrons of boron and ($2s^22p^3$) electrons of nitrogen. The core electrons ($1s^2$) of carbon, boron and nitrogen are replaced by the projector augmented wave (PAW) and pseudopotential approach[17, 18]. A plane-wave

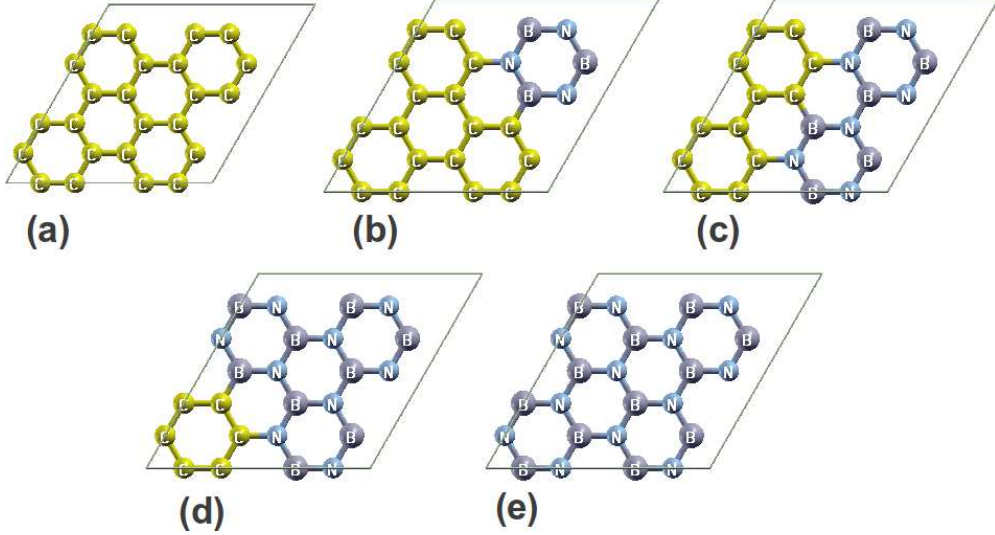


FIG. 1. Atomic structures of five configurations in order of *h*-BN concentration: (a) 0%; (b) 25%; (c) 50%; (d) 75%; (e) 100%.

cutoff of 520 eV is used in all the calculations.

The criterion to stop the relaxation of the electronic degrees of freedom is set by total energy change to be smaller than 0.000001 eV. The optimized atomic geometry was achieved through minimizing Hellmann-Feynman forces acting on each atom until the maximum forces on the ions were smaller than 0.001 eV/Å.

The atomic structures of the five configurations were obtained by fully relaxing a 24-atom-unit cell where all atoms were placed in one plane. The irreducible Brillouin Zone was sampled with a Gamma-centered $19 \times 19 \times 1$ *k*-mesh and initial charge densities were taken as a superposition of atomic charge densities. There was a 14 Å thick vacuum region to reduce the inter-layer interaction to model the single layer system.

The elastic tensor is determined by performing six finite distortions of the lattice and deriving the elastic constants from the stress-strain relationship [19]. The strain applied is ± 0.015 along three major axes for the finite deformations. The elastic constants are obtained from the least-squares extraction of coefficients in stress-strain relationship.

The optimized atomistic structures of the five configurations shown in panels (a)-(e) in Fig. 1 were determined using DFT calculations. The lattice constants are plotted in Fig. 3.

Due to the intrinsic difference between pure *h*-BN and graphene, the lattice constants of the *h*-BNC mixtures are obtained by averaging the lattice vectors of the super-cells. We

found that the lattice constant increases with h -BN concentration C_{BN} . Our results are in good agreement with experiments in h -BN (2.51 Å) [20] and graphene (2.46 Å) [21].

The elastic constants were obtained from DFT calculations. Due to the symmetry, only C_{11} and C_{12} are independent. C_{11} decreases linearly with respect to C_{BN} , as plotted in top panel of Fig. 2. The inplane stiffness Y_s can be obtained from the elastic moduli C_{11} and C_{12} as $Y_s = (C_{11}^2 - C_{12}^2)/C_{11}$. The Poisson's ratio ν which is the ration of the transverse strain to the axial strain can be obtained from elastic moduli as $\nu = C_{12}/C_{11}$. Our result of ν and C of the five configurations are shown in bottom panels of Fig. 2. Our calculated value of inplane stiffness of graphene (355.2 N/m) is in good agreement with the experimental value (340 ± 50 N/m) [22] and theoretical predictions (348 N/m in ref.[23] and 335 N/m in ref. [24]). Our calculated value of Y_s of h -BN (300.3 N/m) agree with *ab initio* (GGA-PW91) prediction (267 N/m in ref. [24]). Poisson's ration ν are 0.16 and 0.18 for graphene and h -BN, agreeing with ref. [24] 0.16 and 0.21 respectively. We found that C_{11} and the inplane stiffness decrease almost linearly as h -BN concentration increase, while C_{12} , as well as Poisson's ration ν , show a rather more complicated behavior Fig. 2. The similar trend of inplane stiffness and C_{11} are based on the fact that C_{11} is dominant, about 6 times bigger than C_{12} . For the same reason, Poisson's ration ν has the similar trend as C_{12} . As a result, we only need to focus on the analysis of C_{11} as follows.

To understand the mechanism of linear elastic properties with respect to the C_{BN} , we studied the electronic charge density $\rho_e = q/S$, where q is the total electronic charge of the system and S the area (cross section) of the system in xy plane. We found that ρ_e monotonically decreases with C_{BN} , as plotted in the top-left panel in Fig. 3. This relationship is consistent with the a - C_{BN} since q is the same in all five configurations. The area mass density $\rho_m = m/S$ (m is the atomic mass) are also studied, as plotted in the bottom-left panel in Fig. 3. ρ_m reaches the minimum at $C_{BN} = 0.5$. The relationship between Y_s and ρ_e was examined and plotted in bottom-right panel of Fig. 3. It is interesting to note that the inplane stiffness monotonically increase with respect to the area charge density ρ_e . It gives a hint that the elastic properties can be engineered by doping or introducing defects which changes the charge densities.

In these h -BNC structures, there is a non-zero stiffness both for volumetric and shear deformations. Hence, it is possible to generate sound waves with different velocities dependent on the deformation mode. Sound waves generating volumetric deformations (compressions)

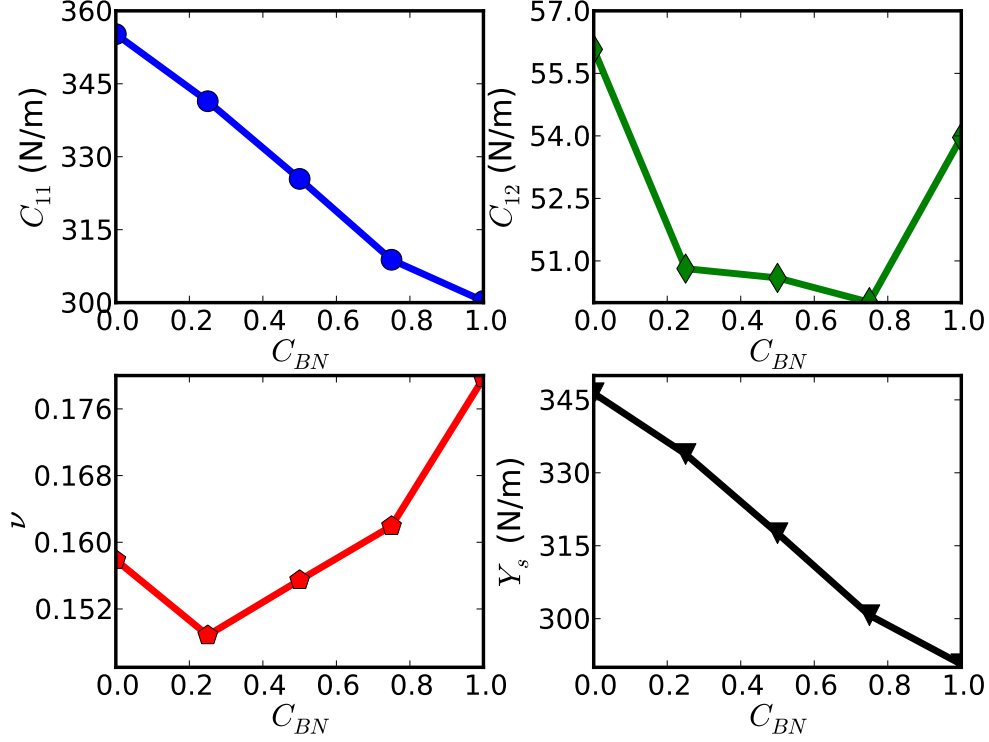


FIG. 2. Elastic constants C_{11} and C_{12} , Poisson's ration ν and inplane stiffness Y_s as a function of h -BN concentrations C_{BN} .

and shear deformations are called longitudinal waves (p -wave) and shear waves (s -wave), respectively. The sound velocities of these two type waves are respectively given by: [25]

$$v_p = \sqrt{\frac{E(1-\nu)}{\rho_m(1+\nu)(1-2\nu)}} \quad (1)$$

$$v_s = \sqrt{\frac{C_{12}}{\rho_m}} \quad (2)$$

The dependent of v_p and v_s on C_{BN} are plotted in Fig. 4. v_p monotonically reduced with C_{BN} while v_s is more complicated. As a rough estimate, the v_p is 3 times of v_s in these h -BNC structures.

In summary, we used *ab initio* density functional theory to investigate the effect of the h -BN domain size on the elastic properties of graphene/ h -BN hybrid monolayers. The elastic constants of five congurations were explicitly examined. We found that the inplane stiffness increases linearly with respect to the h -BN concentrations. This result may provide guidance in practical engineering applications of these nano-heterostructures.

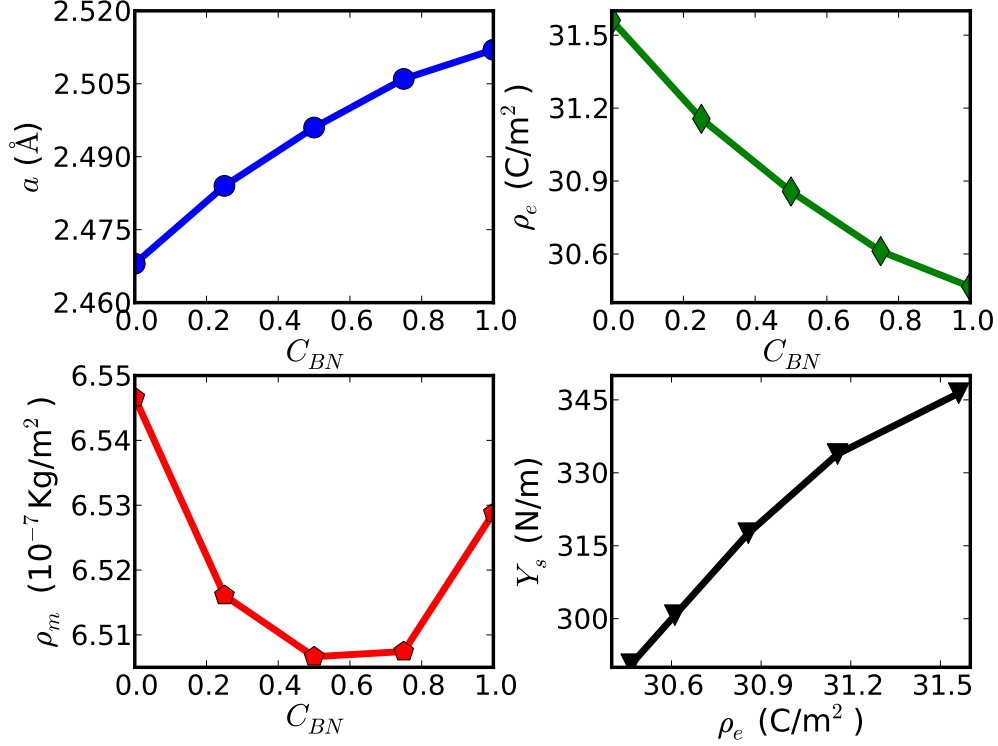


FIG. 3. Lattice constants a , electronic charge density ρ_e and mass density ρ_m as a function of h -BN concentrations C_{BN} . The inplane stiffness Y_s varied with electronic charge density is plotted.

ACKNOWLEDGMENTS

The authors would like to acknowledge the generous financial support from the Defense Threat Reduction Agency (DTRA) Grant # BRBAA08-C-2-0130.

-
- [1] L. Ci, L. Song, C. Jin, D. Jariwala, D. Wu, Y. Li, A. Srivastava, Z. F. Wang, K. Storr, L. Balicas, F. Liu, and P. M. Ajayan, *NATURE MATERIALS* **9**, 430 (MAY 2010).
 - [2] X. Wang, X. Li, L. Zhang, Y. Yoon, P. K. Weber, H. Wang, J. Guo, and H. Dai, *SCIENCE* **324**, 768 (MAY 8 2009).
 - [3] T. B. Martins, R. H. Miwa, A. J. R. da Silva, and A. Fazzio, *Phys. Rev. Lett.* **98**, 196803 (May 2007).
 - [4] A. Lherbier, X. Blase, Y.-M. Niquet, F. m. c. Triozon, and S. Roche, *Phys. Rev. Lett.* **101**, 036808 (Jul 2008).
 - [5] M. Kawaguchi, T. Kawashima, and T. Nakajima, *Chemistry of Materials* **8**, 1197 (1996).

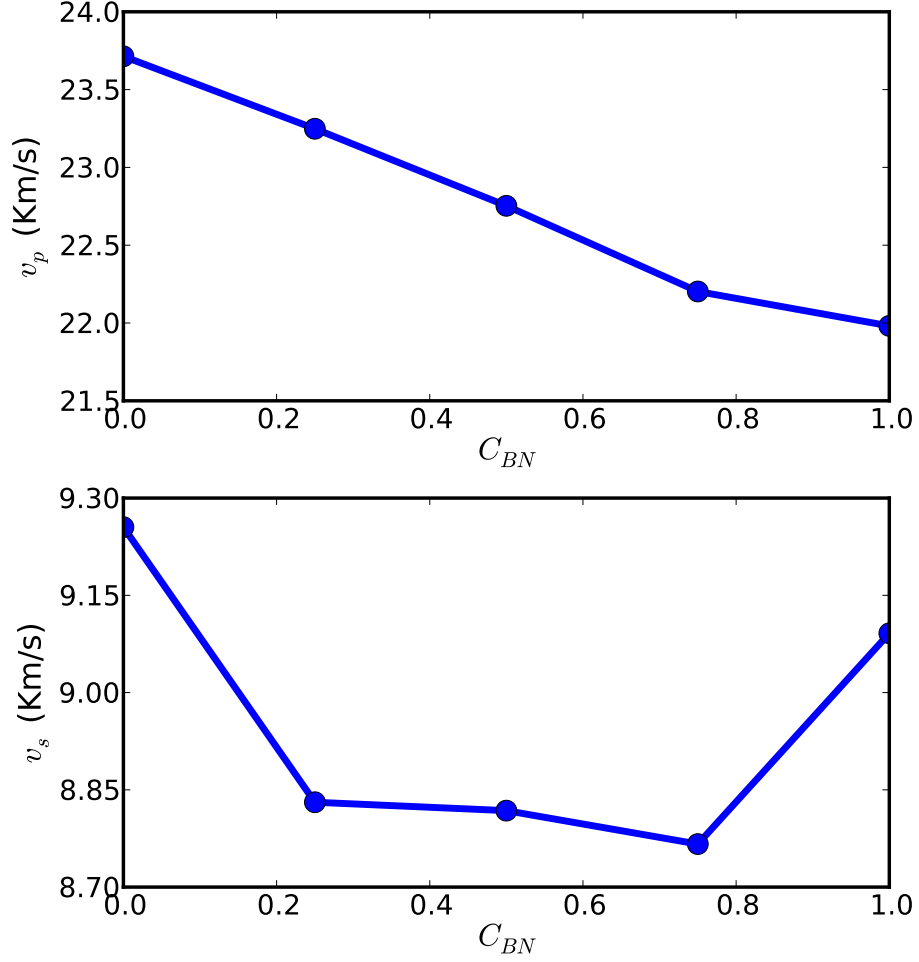


FIG. 4. p -wave and s -wave velocity as a function of h -BN concentrations C_{BN} .

- [6] K. Suenaga, C. Colliex, N. Demoncey, A. Loiseau, H. Pascard, and F. Willaime, *Science* **278**, 653 (1997).
- [7] W.-Q. Han, W. Mickelson, J. Cumings, and A. Zettl, *Applied Physics Letters* **81**, 1110 (2002).
- [8] T. Kawasaki, T. Ichimura, H. Kishimoto, A. A. Akbar, T. Ogawa, and C. Oshima, *SURFACE REVIEW AND LETTERS* **9**, 1459 (JUN-AUG 2002).
- [9] Q. Peng, A. Zamiri, and S. De, *arXiv* **05**, 3776 (2011).
- [10] G. Kresse, , and J. Hafner, *Phys. Rev. B* **47**, 558 (1993).
- [11] G. Kresse and J. Hafner, *Phys. Rev. B* **49**, 14251 (1994).
- [12] G. Kresse and J. Furthuller, *Phys. Rev. B* **54**, 11169 (1996).
- [13] G. Kresse and J. Furthuller, *Comput. Mater. Sci.* **6**, 15 (1996).
- [14] P. Hohenberg and W. Kohn, *Phys. Rev.* **136**, B864 (Nov 1964).

- [15] W. Kohn and L. J. Sham, Phys. Rev. **140**, A1133 (Nov 1965).
- [16] J. Perdew, K. Burke, and M. Ernzerhof, Phys. Rev. Lett. **77**, 3865 (1996).
- [17] P. E. Blöchl, Phys. Rev. B **50**, 17953 (Dec 1994).
- [18] R. O. Jones and O. Gunnarsson, Rev. Mod. Phys. **61**, 689 (Jul 1989).
- [19] Y. Le Page and P. Saxe, Phys. Rev. B **65**, 104104 (Feb 2002).
- [20] L. Liu, Y. P. Feng, and Z. X. Shen, Phys. Rev. B **68**, 104102 (Sep 2003).
- [21] Y. BASKIN and L. MEYER, PHYSICAL REVIEW **100**, 544 (1955), ISSN 0031-899X.
- [22] C. Lee, X. Wei, J. W. Kysar, and J. Hone, SCIENCE **321**, 385 (JUL 18 2008).
- [23] X. Wei, B. Fragneaud, C. A. Marianetti, and J. W. Kysar, PHYSICAL REVIEW B **80**, 205407 (NOV 2009).
- [24] M. Topsakal, S. Cahangirov, and S. Ciraci, APPLIED PHYSICS LETTERS **96** (2010).
- [25] L. E. Kinsler, *Fundamentals of acoustics* (John Wiley & Sons, New York, 2000).